Evaluating Machine Learning & Antenna Placement for Enhanced GNSS Accuracy for CAVs

E. I. Adegoke[1], Jasmine Zidane[1], Erik Kampert[1], Paul A. Jennings[1], Col R. Ford[2], Stewart A. Birrell[1], Matthew D. Higgins[1]

***Abstract*— Localization accuracy obtainable from global navigation satellites systems in built up areas like urban canyons and multi-storey car parks is severely impaired due to multipath and non-line-of-sight signal propagation. In this paper, a simple classifier was used in discriminating between multipath and line-of-sight GNSS signals. By using the carrier to noise ratio which characterizes the received signal strength of the GNSS signals, and the rate of change of the epochs of the satellite vehicles in view, a prediction accuracy of 98% was attained from the classifier. Also investigated in this paper is the effect of antenna placement on localization accuracy. Our measurement campaign using a Nissan Leaf hatch back model showed that the centre longitudinal line of the roof generated the least localization errors for an urbanized route.**

I. INTRODUCTION

Currently, global navigation satellite systems (GNSS) provides huge benefits to a wide range of industries. Some of which are road transportation, finance, agriculture, and public safety which leverage GNSS as a positioning, navigation and timing (PNT) solution [1]. In addition, with the growing interest and adoption of connected autonomous vehicles (CAVs), it is envisaged that GNSS will be adopted for diverse vehicle safety applications in the future [2]. One of the main challenges associated with adopting GNSS is related to localization accuracy in urban canyons. Although GNSS provides an acceptable level of accuracy in open sky areas, its performance degrades severely in dense areas due to multipath propagation. Obstacles such as tall buildings and green foliage result in reducing the localisation accuracy to tens of meters [3].

GNSS is a time-based ranging system where the distance between the transmitter and receiver can be determined by calculating the difference between the signal reception time (ToA) and the signal transmission time (ToT), multiplied with the speed of electromagnetic waves. In order to estimate the 3D position of a user, pseudoranges are required from at least four satellites in view to compensate for the clock bias between the receiver's quartz clock and the transmitter's atomic clock. The pseudorange to satellites can be calculated using (1),

$$\rho^k = \sqrt{(x^k - x) + (y^k - y) + (z^k - z)} \tag{1}$$

where x^k, y^k, z^k represent the k^{th} satellite position and the user position is represented by x,y,z.

The estimation of a user's position, velocity and time (PVT) from a GNSS depends on two main factors, which are: the number and geometry of available satellites in view and the quality of the pseudoranges/Doppler rates [4]. With respect to the spatial arrangement of the satellites in the sky, this changes based on the movement of the satellites in orbit and it's characterized by the dilution of precision (DoP) [5]. Also, errors in the parameters of the navigation (NAV) message, signal propagation delays and signal distortion from several sources can also affect the accuracy of the pseudorange measurement.

Given that GNSS receivers depend on pseudoranges measurements to estimate the user?s absolute position, the ability to classify received signals according to propagation paths would reduce the ranging error to the satellite vehicles. These signals can be classified as multipath and line of sight (LoS) signals. Supervised learning is a widely known machine learning (ML) techniques whereby a training set with known labels/output is used to train a model for the purpose of predicting future outputs [6]. To generalise new instances, either a classifier or a regression is created from the rule of set [7]. Within this subset of ML, some of the mapping forms of the prediction function used include Decision tree (DT), Logistic regression (LR), Neural networks (NN) and support vector machines (SVM). With respect to DT, it is simple to implement, computationally effective and based on the structure of a tree where there are nodes/branches and leaves. While each node represents a function and each leaf represents a classification outcome, in order to make a prediction, a single decision is followed starting from the root node through to the branches. DT can also be implemented as a classification tree with binary labels or as a regression tree with a real numbers as the outcome [8].

The GNSS antenna design is essential to obtaining robust positioning solutions for road vehicles. In the automotive industry, there are precise guidelines relating to the physical characteristics of the antenna and its radiation profile [9]. Moreover, the size of the antenna and its integrity with the car design are considered as constraints that affect the cost and the complexity of the overall design [10]. It also argued that the placement of the GNSS antenna can play

*This work has been sponsored by Innovate UK under grant No. 95143- 564624 with Spirent Communications Plc., WMG and Chronos Technology Ltd. The doctorate of J. Zidan is also supported by Spirent Communications Plc. as part of the Warwick Collaborative Postgraduate Research Scholarships (WCPRS).

[1]E. I. Adegoke, Jasmine Zidane, Erik Kampert, Paul A. Jennings, Stewart A. Birrell and Matthew D. Higgins are with WMG, University of Warwick, Coventry, CV4 7AL, U.K. elijah.adegoke@warwick.ac.uk

[2]Col R. Ford is with Spirent Communications Plc, TQ4 7QR, Paignton, UK

a crucial role to the antenna's performance after integration. For example, the antenna patterns might be affected by metal content present in the car's body [11]. Thus, it is essential that simulation tools are used to study these effects [12]. Alternatively, radio frequency (RF) measurements can be carried out as seen in [13] to pre-empt the behaviour of the radio propagation channel. In order to empirically understand the impact of the GNSS antenna location on a vehicle's roof in terms of obtainable localization accuracy, we have carried out equivalent mobile measurements for various antenna placements.

By using the signal strength as a distinct feature of GNSS signals, a DT algorithm was used to classify the signals received by the antenna into multipath and LoS signals. The remainder of this paper is organized as follows: Section II and III discuss ML and antenna placement with regards to GNSS and CAVs. Section IV describes the data collection process and measurement rig setup. In Section V we present the results and conclude the paper in Section VI.

II. MACHINE LEARNING FOR GNSS

In [14], a combination of features was to classify the positioning accuracy into three categories: Inaccurate, Medium accuracy and High accuracy. The features adopted were the number of satellites in view, signal-to-noise ratio (SNR), DoP, and the speed of the receiver. A standard GPS receiver (SiRF starIII Evaluation Receiver) was attached to a vehicle for collecting real-life GPS data in both open sky and urban canyon. With respect to the analysis and results, three classification methods were compared with the following error rates: principal component analysis (PCA) with error rate of 26%, Hierarchical classification using class unfolding with error rate of 25.33% and a context-based accuracy classification method with an error percentage of 22.17%.

The authors in [15] used a SVM to train a multipath error estimator for a GPS static receiver. A dual channel Trimble NetsRS receiver was used to collect GPS data for five days and the feature set adopted was made up of the satellite elevation and azimuth angles. The results showed that the error estimator enhanced the average standard deviation of the multipath error. By applying support vector regression (SVR) to correct the data set, a 79% performance improvement was observed in the multipath error estimator.

In [16], NN and SVM were used to identify the surrounding environment and the possible multipath scenarios for selecting a receiver tracking strategy. The features used for the multipath scenarios were extracted from the correlation samples of GPS and Galileo signals. The temporal features characterised the surrounding environment as suburban, urban, indoor and open sky and the spectral features were used to identify whether the receiver was a pedestrian or a vehicle. A NovAtel GNSS + INS solution was used as tightly coupled data fusion framework to obtain a reference position solution of 1m accuracy. The framework presented showed a 5% to 35% increase in the accuracy of the estimated RMS (root-mean-square) position error.

SVM was also used in [17] to classify the GNSS pseudorange measurement into three different categories NLoS, LoS and multipath signals. The feature set adopted in this work were the received signal strength and Doppler shift. A fixed u-blox M8 receiver was used to record GNSS signals in dense building environment and ray tracing simulator was used to correctly obtain labelled NLoS signals. Topographic data was used as ground truth and the accuracy of the classifier presented was approximately 75%.

III. GNSS LOCALIZATION & ANTENNA PLACEMENTS

When deciding where to place an antenna on a vehicle, interference with signals from nearby antennas should be minimized using the required separation distance. Moreover, there is a higher possibility of receiving multipath and reflections of the signals near the edges and windows. Consequently, system designers should consider this as it can severely impair the localization accuracy [18].

The authors in [18] investigated the impact of GPS antenna placement on the accuracy of the calculated position. Two Motorola Oncore 8-channels receivers were used to record the data and the reference antenna was placed at the centre of the roof as well as on the dashboard within the cabin. The DoP was used as a feature to estimate the impact of antenna placement on the estimated location accuracy. The analysis presented showed that for optimal performance, the GPS antenna needs to be positioned such that it maximises LoS signals and should be placed on a large ground plane. The results showed that either the centre of the rooftop or the rear centre of the vehicle?s trunk lid are the best locations to place a GPS antenna. It was also highlighted that placing the antenna inside the car negatively affects its performance.

The theory of characteristics modes was used to study the placement of a monopole antenna on the metallic rooftop of a vehicle in [11]. Along the longitudinal centre line of the vehicle, the final third towards the rear of the roof was determined to be the optimal position. In [19], the authors investigated the effect of antenna placement on the precise positioning of a low-cost GNSS receiver (with a patch antenna). A comparison between two identical u-blox receivers was also presented; with one placed on the roof of the vehicle and the other was placed on the dashboard inside the cabin. In order to obtain precise positioning information, a Leica Viva GS15 GNSS receiver was installed on the roof. The carrier to noise ratio (C/N_o) and the circular error probable (CEP) were used as figure of merit. The results showed that the antennas mounted on the car's roof performed better and 90% of the CEPs were reduced by several meters.

IV. GNSS DATA PROCESSING, ROVER SETUP & MEASUREMENT SCENARIOS

A. Learning Data Collection & Processing

Since GNSS observation sites are positioned to receive unobstructed radio propagation paths from satellite vehicles, we obtained LoS data samples for the learning algorithm from an online GPS/GNSS database. The LoS data used in

training the learning algorithm was taken from a 24-hour observation (obs) RINEX file for January 1, 2018 [20] and multipath signals were obtained from a 24 hour recording via a u-blox receiver. This was easily carried out by placing the u-blox outside the window of a residential apartment in Coventry, UK. The data labels adopted were: "label 1" for data obtained from the observation site and "label 0" for u-blox data representing multipath and NLoS.

With respect to data labelling and training, only GPS L1 C/N_o was extracted from both Rinex files. Thus, according to RINEX file naming, the parameter "S1" from the satellite vehicles present was processed. The RINEX files were read using a python RINEX file reader [21], and the content of the observation files were edited to remove SBAS and GLONASS using *TEQC* [22]. Subsequently MATLAB scripts were written to extract and preprocess the data. Regarding the data samples, 57760 samples were obtained from the observation site and 45832 samples from the u-blox receiver. Prior to implementing the learning algorithm, the feature set was scaled using min-max normalization (as shown in (2)), randomized and then split using a 90/10 training/test rule.

$$x' = \frac{x - \min(x)}{\max(x) - \min(x)} \tag{2}$$

For each satellite vehicle present at each site, the rate of change of C/N_o ($\Delta C/N_o$) was obtained using (3)

$$\Delta cn_j^k = cn_{j+1}^k - cn_j^k \tag{3}$$

where k is the index of the GPS satellite vehicle and j represents the epochs in the RINEX files. It should be noted that the sampling interval of the GNSS data recording determines the amount of data recorded per site.

B. Rover Setup and Measurement Scenario

A u-blox (NEO-M8T) breakout receiver board and a AeroAntenna Technology AT1675 GNSS wideband antenna were used in recording GNSS signals in this work. The specifications of the setup are summarized in Table I. With respect to the antenna placement, the GNSS antenna was mounted at the grid intersections on the roof of a Nissan Leaf 2011 model as shown in Figs. 1 and 2. In total, eighteen (18) antenna positions were used with 27.5cm spacing between each grid point. The measurement scene was a University campus, which had environments that fit urban canyons, sparse and dense foliage as well as outdoor car parks. The weather during the measurement campaign was overcast with clear sky.

V. Evaluation and Results

A. Evaluating Classification Learning Results

In order to evaluate the performance of the DT algorithm, we used the prediction accuracy as a figure of merit. Given the layout of the data points on a scatter plot and the need for a simple learning technique, we adopted the decision tree (DT) algorithm which used the C/N_o and $\Delta C/N_o$ as a feature set. Within the DT algorithm, Fine, Medium and Coarse DT

TABLE I

Rover Setup Specifications

Parameter	Value
Antenna	
Frequency	1164 - 1295 MHz, 1525 - 1615 MHz
GNSS Bands	GPS L1/L2/L5, Compass B1/B2/B3, GLONASS G1/G2, Galileo E5a/E5b
Polarization	Right hand circular
Gain	39 dB
Impedance	50 Ohms
VSWR	$\leq$2.0:1
Receiver	
GNSS Bands	GPS/QZSS L1 C/A, GLONASS L10F, BeiDou B1 SBAS L1 C/A: WAAS, EGNOS, MSAS Galileo-ready E1B/C
Position accuracy	2.5m CEP

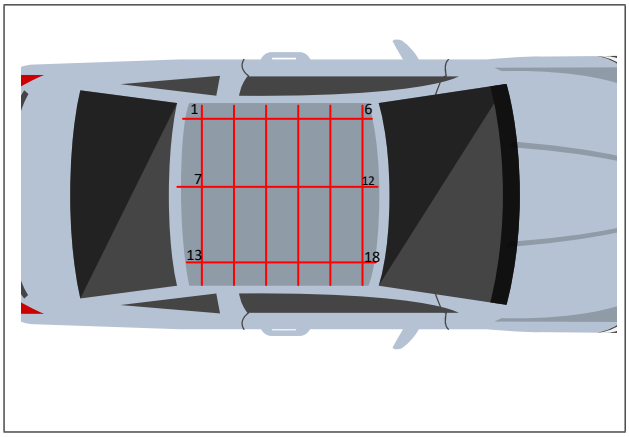

Fig. 1. Depiction of the antenna locations on the Nissan Leaf

TABLE II

Accuracy of Decision Tree Algorithms

	Coarse DT (%)	Medium DT (%)	Fine DT (%)
Training	91.90	95.10	98.90
Test	92.30	95.12	98.75

were used to train the model. In Table II, the prediction accuracy obtainable for each method is presented. In Fig 3, the coarse DT model is depicted, where *column_1* represents C/N_o and *column_2* represents $\Delta C/N_o$. With respect to the Medium and Fine DT, pruned versions are shown in Figs. 4 and 5. Intuitively, the accuracy increases with the DT levels. In general, it can be observed that the $\Delta C/N_o$ of subsequent epochs for multipath signals is higher than that of LoS signals [17].

B. Evaluating Antenna Placement and Localization Accuracy

In Table III, the root mean square error (RMSE) of the localization accuracy is presented. The displacement between the observed and truth positions was obtained by using the Haversine formula shown in (4),

$$a = \sin^2(\Delta Lat/2) + \cos(Lat1)\cos(Lat2)\sin^2(\Delta Lon/2) \tag{4a}$$

Fig. 2. GNSS antenna mounted on a Nissan Leaf 2011

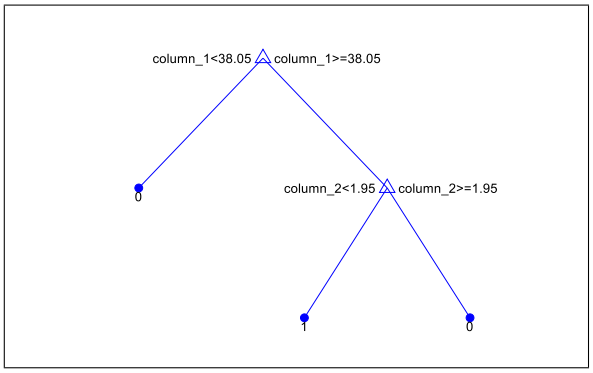

Fig. 3. Coarse Decision Tree Model

$$c = 2\,\mathrm{atan2}(\sqrt{a}, \sqrt{(1-a)}) \tag{4b}$$

$$d = R.c \tag{4c}$$

where ΔLat and ΔLon are the difference in latitude/longitude of the points, R is the radius of the earth and d is the calculated distance. In this work, the road markings as depicted in Google Maps were used as truth positions. The results show that the antenna locations with the least errors are located along the longitudinal mid section of the car, which aligns with the literature [11]. Points 8 and 11 (as depicted in Fig 1), which are approximately equidistant from the start and end of the car's roof show the least errors. The results also show that the grid line on the driver's side generated lower errors when compared with the extreme left grid. This can be associated with the left-hand traffic (LHT) rule of the road, as the driver's side has a better view since it's further away from the buildings. Nonetheless, this grid line is affected by reflections from moving vehicles when compared to the middle grid line. With respect to the topography of the campus, localization errors as high as 30m were recorded at the bends shown in Fig. 6. This is as a result of the buildings and dense foliage close to the road, which obscures the sky view of the antenna.

TABLE III
SUMMARY OF LOCALIZATION ACCURACY

Location index	RMSE (m)
1	9.93
2	11.67
3	8.52
4	8.38
5	10.52
6	8.82
7	7.10
8	6.66
9	10.70
10	10.16
11	7.16
12	8.52
13	10.69
14	8.39
15	7.73
16	10.00
17	9.01
18	11.68

VI. CONCLUSIONS

Localization accuracy obtainable from an off the shelf component has been characterized in this work within a typical urban environment. From a system integration point of view, the results presented in this work show that the external placements of antennas on a vehicle for the purpose of positioning affects the accuracy obtainable. From our results, it is recommended that the antenna be placed along the longitudinal mid way section and approximately one-third from the front or back of the car's roof. Since the propagation conditions of a signal affects the ranging and localization accuracy, a simple classification method using signal strength thresholds was evaluated in this work. By using the signal strength and change in the signal strength of subsequent epochs from visible satellite vehicles, the decision tree algorithm was able to attain an accuracy of approximately 98%.

REFERENCES

[1] European Global Navigation Satellite Systems Agency, "GNSS Market Report." [Online]. Available:https://www.gsa.europa.eu/system/files/reports/gnss_mr_2017.pdf

[2] X. Meng, S. Roberts, Y. Cui, Y. Gao, Q. Chen, C. Xu, Q. He, S. Sharples, and P. Bhatia, "Required navigation performance for connected and autonomous vehicles: where are we now and where are we going?" *Transportation Planning and Technology*, vol. 41, no. 1, pp. 104–118, 2018.

[3] R. T. Ioannides, T. Pany, and G. Gibbons, "Known vulnerabilities of global navigation satellite systems, status, and potential mitigation techniques," *Proceedings of the IEEE*, vol. 104, no. 6, pp. 1174–1194, June 2016.

[4] P. Misra and P. Enge, *Global Positioning System: Signals, Measurements, and Performance*. Ganga-Jamuna Press, 2011. [Online]. Available:https://books.google.co.uk/books?id=5WJOywAACAAJ

[5] O. Elmasry, M. Tamazin, H. Elghamarawy, M. Karaim, A. Noureldin, and M. Khedr,"Examining the benefits of multi-gnss constellation for the positioning of high dynamics air platforms under jamming conditions," in *2018 11th International Symposium on Mechatronics and its Applications (ISMA)*, March 2018, pp. 1–6.

[6] S. B. Kotsiantis, "Supervised machine learning: A review of classification techniques," in *Proceedings of the 2007 Conference on Emerging Artificial Intelligence Applications in Computer Engineering: Real Word AI Systems with Applications in eHealth, HCI, Information Retrieval and Pervasive Technologies*. Amsterdam, The

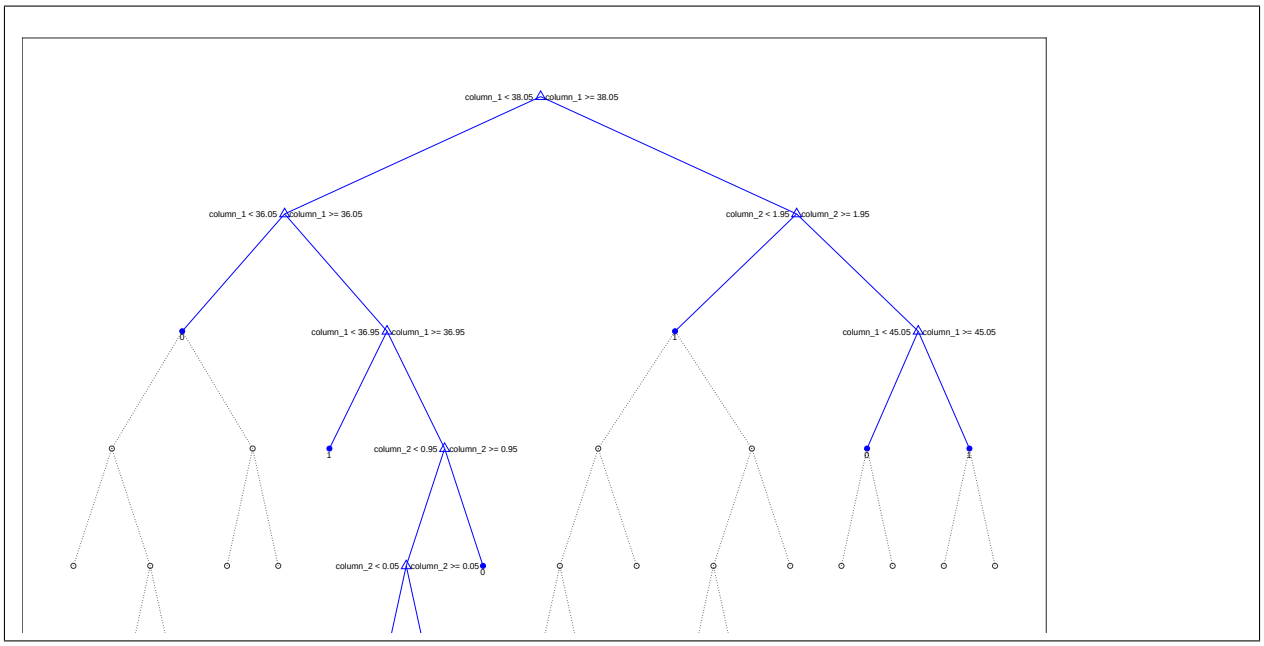

Fig. 4. Medium Decision Tree Model with Pruning level 7/11

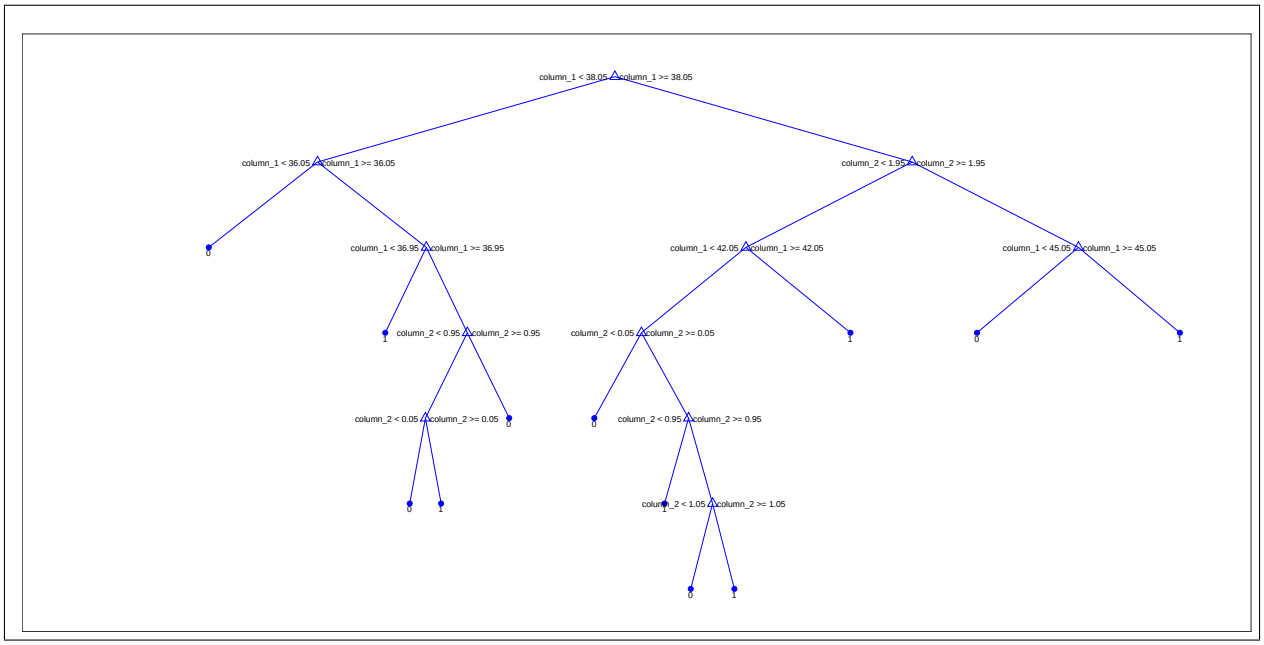

Fig. 5. Fine Decision Tree Model with Pruning level 28/33

Netherlands, The Netherlands: IOS Press, 2007, pp. 3–24. [Online]. Available:http://dl.acm.org/citation.cfm?id=1566770.1566773

[7] N. Linty, A. Farasin, A. Favenza, and F. Dovis, "Detection of gnss ionospheric scintillations based on machine learning decision tree," *IEEE Transactions on Aerospace and Electronic Systems*, pp. 1–1, 2018.

[8] L. Breiman, J. Friedman, C. Stone, and R. Olshen, *Classification and Regression Trees*, ser. The Wadsworth and Brooks-Cole statistics-probability series. Taylor & Francis, 1984. [Online]. Available: https://books.google.co.uk/books?id=JwQx-WOmSyQC

[9] European Global Navigation Satellite Systems Agency, "GNSS User Technology Report." [Online]. Available:https://www.gsa.europa.eu/european-gnss/gnss-market/gnss-user-technology-report

[10] "Cst-computer simulation technology." [Online]. Available:https://www.cst.com/events/webinars/2014-11-04-antenna-design

[11] J. Yang, J. Li, and S. Zhou, "Study of antenna position on vehicle by using a characteristic modes theory," *IEEE Antennas and Wireless Propagation Letters*, vol. 17, no. 7, pp. 1132–1135, July 2018.

[12] M. Rutschlin and D. Tallini, "Simulation for antenna design and placement in vehicles," in *Antennas, Propagation RF Technology for Transport and Autonomous Platforms 2017*, Feb 2017, pp. 1–5.

[13] E. Kampert, P. A. Jennings, and M. D. Higgins, "Investigating the v2v millimeter-wave channel near a vehicular headlight in an engine bay," *IEEE Communications Letters*, vol. 22, no. 7, pp. 1506–1509, July 2018.

[14] N. M. Drawil, H. M. Amar, and O. A. Basir, "Gps localization accuracy classification: A context-based approach," *IEEE Transactions on Intelligent Transportation Systems*, vol. 14, no. 1, pp. 262–273,

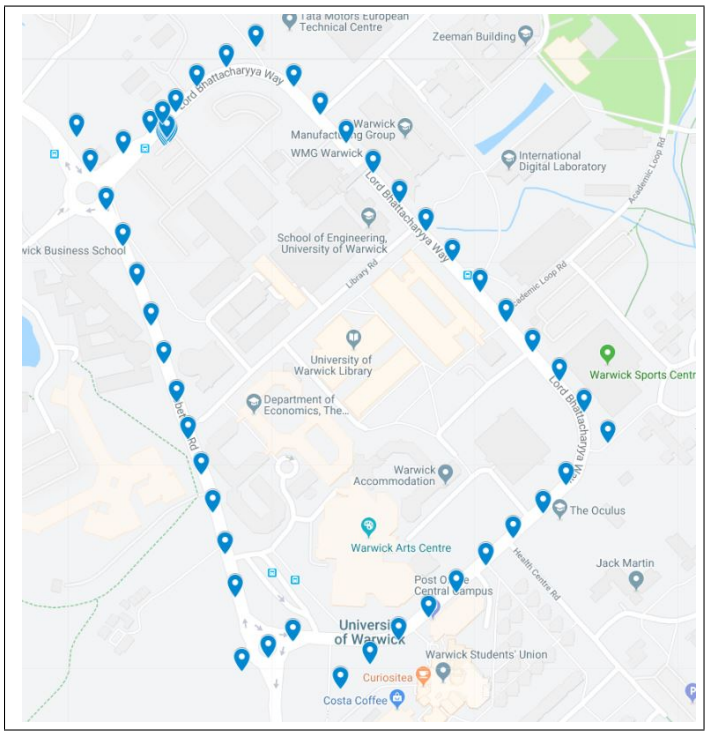

Fig. 6. Measurement test route positions for antenna location 5

March 2013.

[15] Q.-H. Phan, S.-L. Tan, and I. Mcloughlin, "Gps multipath mitigation: A nonlinear regression approach," *GPS Solut.*, vol. 17, no. 3, pp. 371–380, Jul. 2013. [Online]. Available:http://dx.doi.org/10.1007/s10291-012-0285-5

[16] N. Sokhandan, A. Broumandan, and G. Lachapelle, "Gnss multipath mitigation using low complexity adaptive equalization algorithms," in *5th ESA International Colloquium Scientific and Fundamental Aspects of the Galileo Programme Physikalisch-Technische Bundesanstalt (PTB)*, Oct 2015. [Online]. Available:https://schulich.ucalgary.ca/labs/position-location-and-navigation/node/254

[17] L. Hsu, "Gnss multipath detection using a machine learning approach," in *2017 IEEE 20th International Conference on Intelligent Transportation Systems (ITSC)*, Oct 2017, pp. 1–6.

[18] Y. Dai, T. Talty, and L. Lanctot, "Gps antenna selection and placement for optimum automotive performance," in *IEEE Antennas and Propagation Society International Symposium. 2001 Digest. Held in conjunction with: USNC/URSI National Radio Science Meeting (Cat. No.01CH37229)*, vol. 1, July 2001, pp. 132–135 vol.1.

[19] M. Kirkko-Jaakkola, S. Feng, Y. Xue, X. Zhang, S. Honkala, S. Soderholm, L. Ruotsalainen, W. Ochieng, and H. Kuusniemi, "Effect of antenna location on gnss positioning for its applications," in *2016 European Navigation Conference (ENC)*, May 2016, pp. 1–7.

[20] K. Hudnut, N. King, A. G. Aspiotes, A. A. Borsa, G. Determan, Daniel N., J. E., and K. F. Stark, "SCIGN USGS GPS Network - 7ODM-Seven Oaks Dam P.S., UNAVCO, GPS/GNSS Observations." [Online]. Available:https://doi.org/10.7283/T5M32T1K

[21] H. Michael, "Georinex." [Online]. Available:https://github.com/scivision/georinex

[22] L. H. Estey and C. M. Meertens, "Teqc: The multi-purpose toolkit for gps/glonass data," *GPS Solutions*, vol. 3, no. 1, pp. 42–49, Jul 1999. [Online]. Available:https://doi.org/10.1007/PL00012778